LAWRENCE
LIVERMORE
NATIONAL
LABORATORY

UCRL-JRNL-204811

First-order Isostructural Mott transition in highly-compressed MnO

Choong-Shik Yoo

June 21, 2004

First-order Isostructural Mott transition in highly-compressed MnO

UCRL-JRNL-204811

First-order Isostructural Mott transition in highly-compressed MnO

C. S. Yoo, B. Maddox, J.-H. P. Klepeis, V. Iota, W. Evans, and A. McMahan,

Lawrence Livermore National Laboratory, Livermore, California 94551

M. Hu, P. Chow, M. Somayazulu, and D. Häusermann,

HP-CAT, Advanced Photon Source, Chicago, Illinois 60637

R.T. Scalettar and W. E. Pickett

University of California, Davis, California 95616

Abstract

We present evidence for an isostructural, first-order Mott transition in MnO at 105±5 GPa, based on high-resolution x-ray emission spectroscopy and angle-resolved x-ray diffraction data. The pressure-induced structural/spectral changes provide a coherent picture of MnO phase transitions from paramagnetic B1 to antiferromagnetic distorted B1 at 30 GPa, to paramagnetic B8 at 90 GPa, and to diamagnetic B8 at 105±5 GPa. The last is the Mott transition, accompanied by a complete loss of magnetic moment, a ~6.6 % volume collapse and a visual appearance change to metallic luster consistent with recent resistivity measurements.

PACS numbers: 62.50+p, 61.10.-I, 64.70.Kb, 64.30.+t

Mott's seminal work on how insulating character may arise out of the electron-electron repulsion used a *3d* transition metal monoxide, NiO, as an example and suggested its pressure-induced metallization, the Mott transition [1]. Yet for 55 years the Mott transition in the heavier *3d* monoxides has eluded detection at room temperature due to the high pressures required. Recent resistivity measurements using "designer" diamond anvils, however, have seen this insulator-metal transition in MnO, a five order of magnitude decrease in resistivity between 90 and 106 GPa [2]. MnO is a paramagnetic insulator in the B1 (rock salt) structure at ambient pressure and temperature, transforms to an antiferromagnetic rhombohedral distortion (denoted dB1) at 30 GPa, then to an unknown "intermediate" phase at 90 GPa, and then to the B8 (NiAs) structure at around 120 GPa [3]. There is considerable geophysical interest in FeO, which has been metallized for temperatures greater than 1000 K at pressures above 70 GPa [4]. The B8 phase is encountered at 600 K (90 GPa) and above, although FeO remains insulating and in the dB1 phase up to 220 GPa at 300 K, perhaps for kinetic reasons [5]. A magnetic anomaly at 90 GPa in Mössbauer measurements [6] was later identified as a Néel transition [7] while the moment in FeO persists to at least 143 GPa [7]. Transitions from the B1 to two different, successive rhombohedral phases have been seen in CoO [8]. While there may be signs of metallic luster near 100 GPa in NiO, this behavior has yet to be confirmed [9]. High-spin to low-spin transitions have been predicted for all of the *3d* monoxides [10] and the B8 and a variant predicted for compressed MnO and FeO, respectively [11].

It is the purpose of this paper to present new x-ray diffraction and x-ray emission spectroscopy results which suggest that the Mott transition in MnO is a far richer phenomenon than just the onset of metallization. Our results are consistent with a transition at 105±5 GPa in MnO in which there are concurrently: (1) a first-order isostructural transition in the B8 phase with a ~6.6 % volume change, (2) a complete loss of magnetic moment, and (3) the insulator-metal transition as previously noted [2]. The complete magnetic and structural sequence we suggest is consistent with the available data for FeO and may shed light on the later *3d* monoxides as well.

High purity MnO powder samples (99+%, Alfa-Aesar) were loaded in diamond anvil cells together with mineral oil. Mineral oil provides a reasonable quasi-hydrostatic condition, important for probing subtle structural/spectral changes in MnO at high pressures. The ruby spectrum of the sample remains relatively sharp with well-resolved R_1 and R_2 lines at least to 100 GPa above which the lines get rapidly broadened. The pressure was determined at the same spot before and after each x-ray spectral measurement, showing a relatively small pressure difference well within 2 GPa at all pressures. We used beveled diamond anvils (100 μm flat over 300 μm culet) with a relatively small sample chamber (~50 μm hole) in a ~30 μm thick gasket made of either Re for x-ray diffraction or x-ray translucent Be for x-ray emission spectroscopy.

X-ray emission spectroscopy (XES) experiments were done by using intense monochromatic x-rays (10.225 KeV) from an undulator at the 16IDD at the APS. The incident x-ray was focused to ~20 x 50 μm at the sample by using a pair of 1m-long K-B focusing mirrors. X-ray fluorescence was then collected at 90 degree from the incident x-ray to reduce the elastically scattered background, by using a 1-m Rowland circle spectrometer arranged on a vertical plan. A spherically bent Si(333) single crystal analyzer (100 mm in diameter) was used to refocus the fluorescence onto a Si detector (Amp Tek). The Bragg angle is 66.06 degree at the Kβ emission energy 6.490 KeV. The energy calibration has been done using Mn foil. This configuration provides approximately 0.5 eV energy resolution.

Angle-dispersive x-ray diffraction experiments were done by using microfocused (~10 μm) monochromatic (0.3678 Å) x-rays at the 16IDB at the APS. The x-ray diffraction patterns were recorded on an on-line image plate, and the Debye-Scherrer diffraction image was then analyzed by using the FIT2D and GSAS programs.

Kβ emissions of MnO represent transitions associated with the *1s* core-hole decays to the *3p* states in Mn, which consist of two branches ^{7}P and ^{5}P split by about 16 eV as a result of the *3p* core-hole *3d* electron exchange interaction [12]. Therefore, the energy separation and the intensity ratio of two bands are proportional to the magnitude of electron exchange interaction and the net spin of *3d* bands, respectively. Most

significantly, the intensity of the Kβ' band is sensitive to local magnetic moment, as has been well established in many *3d* transition metals and transition metal compounds [13].

Figure 1 illustrates the pressure-induced change of Kβ XES spectra in MnO to 132 GPa. These spectra are overlaid in three groups depending on pressure: the first below 30 GPa with distinctive Kβ' intensity, the second between 40 and 98 GPa where the Kβ' intensity is substantially reduced yet apparent, and the third above 108 GPa where the Kβ' line essentially disappears. It is also apparent that the peak position of the $K\beta_{1,3}$ band is shifted toward lower energy by about 1 eV as the pressure increases from one to the other group. A similar shift of the $K\beta_{1,3}$ peak was also observed in FeO, but was unexplained [7].

It is important to note that these pressure-induced spectral changes are subtle but occur abruptly at 30-40 and 98-108 GPa. Figure 2 plots the peak position of $K\beta_{1,3}$ and the normalized intensity of Kβ' to $K\beta_{1,3}$, clearly showing the evidence for two first-order electronic phase transitions at 35±5 GPa and 103±5 GPa. Also noticed is a small shift of the $K\beta_{1,3}$ below 30 GPa and above 108 GPa, while it remains nearly unchanged between 40 and 98 GPa. The normalized Kβ' intensity between 1 and 30 GPa is about twice of that between 40 and 98 GPa. Above 108 GPa, it again disappears, indicating a complete loss of magnetic moment in this material.

Note that the first discontinuity in XES spectra (Figs. 1 and 2) occurs at the onset of the B1 to dB1 structural phase transition at 30 GPa, but the second occurs near 103 GPa in the middle of "intermediate" phase. Apparently, the first transition is due to the decrease of magnetic moment associated with the transition from paramagnetic B1 to antiferromagnetic dB1, behavior which has been seen theoretically [14]. This result then indicates that the Néel temperature T_N increases to 300 K at 30 GPa, from 118 K at ambient pressure [15]. The pressure-induced T_N increase implies an increase of electron exchange interaction, which can be attributed to the pressure-induced decrease of Mn-Mn interatomic distance. On the other hand, the second electronic phase transition near 103 GPa occurs above 90 GPa where the dB1 transforms to the "intermediate" phase, but below 120 GPa where the "intermediate" phase transforms to the B8 phase. It is possible that this discrepancy is due to the ill-characterized "intermediate" phase.

The present diffraction results (Fig. 3) indicate MnO transforms from the B1 to the dB1 phase at 30 GPa, to "intermediate" at 90 GPa, and to B8 at around 120-130 GPa, similarly to the previous report [3]. However, the present data further reveal that the "intermediate" phase can be interpreted in terms of a mixture between dB1 and B8 phases. All diffraction lines at 90 GPa in Fig 3 are accounted for by either dB1 or B8 with an exception near the broad 102 reflection of dB1. This broad feature, on the other hand, can be easily understood in terms a superlattice reflection (1/2, 1/2, 5/2) near the 102 reflection arising from lattice distortion across the displacive dB1 to B8 phase transition. The refined intensities are well matched to the measured ones for all three phases.

There is only a small difference between dB1 and B8 structures: the dB1 is a six-layer structure A(O)c'(Mn)B(O)a'(Mn)C(O)b'(Mn), whereas the B8 is a four-layer a(Mn)B(O)a(Mn)C(O). Therefore, the dB1 to B8 transition requires a slight displacement of oxygen atoms from distorted octahedral sites with three quasi-nearest Mn-O distances, 1.70, 2.24 and 2.17 Å to perfect trigonal prism sites with all equal Mn-O distance, 2.04 Å. Such a displacive transition between two energetically similar structures often results in relatively large hysteresis in pressure and thus in two phases to consist over an extended pressure range. The examples of similar displacive transitions resulting in commensurate mixtures and superlattice structures are numerous, particularly of electronically driven phase transitions such as the *s-d* electronic phase transitions in alkali metals [16,17], the ferromagnetic-to-nonmagnetic transition in Co [18], the insulator-metal transition in I_2 [19], and other examples of Mott transitions in Fe_2O_3, FeI_2 and NiI_2 [20,21].

Figure 4 shows the present pressure-volume results, with a mixture model used to obtain the specific volumes of dB1 and B8 phases in the intermediate pressure region between 90 and 120 GPa. The specific volume of dB1 decreases seamlessly without apparent discontinuity across the transition at 90 GPa. The B8 phase has nearly the same specific volume as the dB1 at 90 GPa, but becomes about 4.5 % more dense by 110 GPa. Furthermore, the compression curve of B8 phase exhibits a discontinuous volume change of ~ 6.6 % at around 110 GPa, that is a first-order isostructural transition within the B8

phase. A similar discontinuous change is also apparent in the c/a ratio of B8 structure (Fig. 4, inset).

The present spectral and diffraction data together with recent resistivity measurements [2] provide a coherent picture of the Mott transition in MnO. In addition to the isostructural volume collapse at ~ 110 GPa, recall that MnO loses the Kβ' intensity completely above 103±5 GPa, and the resistivity data [2] exhibit a sharp (nearly three orders of magnitude drop) from 10^{1} Ω at 103 GPa to 10^{-2} Ω at 105 GPa. Our visual inspections are consistent with the MnO sample dark and insulator-like near 88 GPa, and then subsequently showing a metallic luster above about 108 GPa. These pressures are all close enough that it seems likely that these three signatures may all be manifestations of the same pressure-induced Mott transition in MnO: isostructural volume collapse, moment collapse (loss or screening), and the insulator-metal transition.

Beginning at atmospheric pressure, we suggest the following sequence of phases as room-temperature MnO is compressed: PM B1 — AFM dB1 — PM B8 — DM B8; where PM, AFM, and DM signify paramagnetic, antiferromagnetic, and diamagnetic; and the transition pressures are 30, 90, and 105±5 GPa, respectively. This sequence exhibits the two essential magnetic features proposed for the temperature-pressure phase diagram of FeO [7], namely passing into and then out of the dome of AFM order which exists below a maximum Néel temperature at some finite pressure, and then moment collapse occurring at still higher pressures in the PM–DM transition. These authors identified the 90 GPa Mössbauer signature [6] for FeO as the high-pressure exit from the region of AFM order [7]. The present structural sequence is also the same B1—dB1—B8 proposed for FeO, and although kinetic effects appear to be impeding the latter transition in FeO at room temperature, this is not the case above 600 K [7].

It is worth noting that a precedent exists in the *f*-electron metals for the coincidence of volume collapse, moment collapse, and insulator-metal transition—with the later redefined as rapid grown of *f* spectral weight at the Fermi level [23]. Indeed, the similarity between the *3d* monoxide series and these electron-correlation-driven transitions in the *f*-electron metals was emphasized years ago [23], and from Fig. 6 of [22] one might expect MnO to be the first of the later monoxides to undergo the collapse

under pressure. It has been argued that a proper treatment of dynamical electron correlations is essential to a full understanding of these unique transitions in both kinds of systems [24], whereas local density techniques as well as their "GGA" and "LDA+U" improvements behave more like static mean field theories in which magnetic moments require concurrent magnetic order, which is inconsistent with phases like the PM B8.

In summary, we have presented MnO phase transitions from PM B1 to AFM dB1 at 30 GPa, to what is likely PM B8 at 90 GPa, and finally to DM B8 above 105±5 GPa. Remnant traces of the dB1 phase appear well above 90 GPa, up to 120-130 GPa. Our combined crystallographic and spectroscopic results together with earlier resistivity measurements [2] raise the tantalizing prospect of a Mott transition in MnO at 105±5 GPa which involves concurrent isostructural volume collapse of ~ 6.6 %, moment collapse, and insulator-metal transition.

We thank Dr. Chi-Chang Kao for lending us his Si analyzer. This work has been supported by the LDRD-04-ERD-020 and PDRP programs at the LLNL, University of California, under the auspices of the U.S. DOE under Contract No. W-7405-ENG-48 and by the Stockpile Stewardship Academic Alliances Program under grant DOE DE-FG03-03NA00071.

References:

1. M. F. Mott, Proc. Phys. Soc. A **62**, 416 (1949); *Metal Insulator Transitions* (Tayor and Francis, London, 1990)
2. J. R. Patterson *et al.*, Phys. Rev. B, in press (2004)
3. T. Kondo *et al.*, J. Appl. Phys. **87**, 4153 (2000)
4. E. Knittle and R. Jeanloz, Geophys. Res. Lett. **13**, 1541 (1986)
5. H.K. Mao *et al.*, Phys. Earth Planet. Inter. **96**, 135 (1996)
6. M. P. Pasternak *et al*, Phys. Rev. Lett. **79**, 5046 (1997).
7. J. Badro *et al.*, Phys. Rev. Lett. **83**, 4101 (1999).
8. Q. Guo *et al.*, J. Phys: Condens. Matter **14**, 11369 (2002).
9. A. Shukla *et al.*, Phys. Rev. B **67**, 081101(R) (2003)
10. R. E. Cohen, I. I. Mazin, D. G. Isaak, Science **275**, 654 (1997)
11. Z. Fang *et al.*, Phys. Rev. Lett. **81**, 1027 (1998); also, Phys Rev. B **59**, 762 (1999)
12. F. deGroot, Chem. Rev. **101**, 1779 (2001)
13. G. Peng *et al.*, J. Am. Chem. Soc. **116**, 2914 (1994)
14. T. Paiva *et al.*, Phys. Rev. B**63**, 125116 (2001)
15. D. Block, C. Vettier, P. Burlet, Phys. Lett. A **75**, 301 (1980)
16. U. Schwartz *et al.*, Phys. Rev. Lett. **81**, 2711 (1998)
17. N. E. Christensen and D. L. Novikov, Solid State Comm. **119**, 477 (2001)
18. C. S. Yoo *et al.*, Phys. Rev. Lett. **84**, 4132 (2000)
19. K. Takemura *et al.*, Nature **423**, 971 (2003)
20. M.P. Pasternak *et al.*, Phys. Rev. Lett. **82**, 4663 (1999).
21. G.Kh. Rozenberg *et al.*, Phys. Rev. B **68**, 64105 (2003)
22. A.K. McMahan *et al.*, J. Comput.-Aided Mater. Design **5,** 131 (1998); cont-mat/9805064

23. B. Johansson, Phys. Rev. B **15**, 5890 (1977)

24. K. Held, *et al.,* Adv. Solid State Phys. **43,** 267 (2003)

Figure Captions:

Fig. 1 Kα x-ray emission branches of MnO at high pressures (all in GPa), showing subtle but apparent spectral changes above 30 GPa and 98 GPa. Nearly disappearing intensity of Kα' line above 108 GPa clearly indicates a complete loss of magnetic moment.

Fig. 2 The pressure-induced spectral changes of MnO as a function of pressure, illustrating two first-order electronic phase transitions at 30 GPa and 103 GPa. The former occurs at the onset of the B1 $\rightarrow$ dB1 transition, whereas the latter occurs within the B8 structure proceeding the dB1 $\rightarrow$ B8 transition at 90 GPa.

Fig. 3 The measured (blue crosses) and refined (red lines) X-ray diffraction patterns of MnO phases: (a) B1 at 25 GPa, (b) dB1 at 45 GPa, (c) dB1+B8 at 90 GPa, and (d) B8 at 161 GPa. Miller indices are marked for each phase, together with the 111 reflection of Cu used as an internal pressure marker.

Fig. 4 The specific volume and the c/a ratio (in the inset) of MnO phases as a function of pressure. Note the discontinuous changes of the specific volume and the c/a ratio at 110 GPa, indicating that MnO undergoes an isostructural phase transition with 6.6 % volume collapse. This transition apparently occurs at the onset of the Mott insulator-metal transition (see Fig. 2).

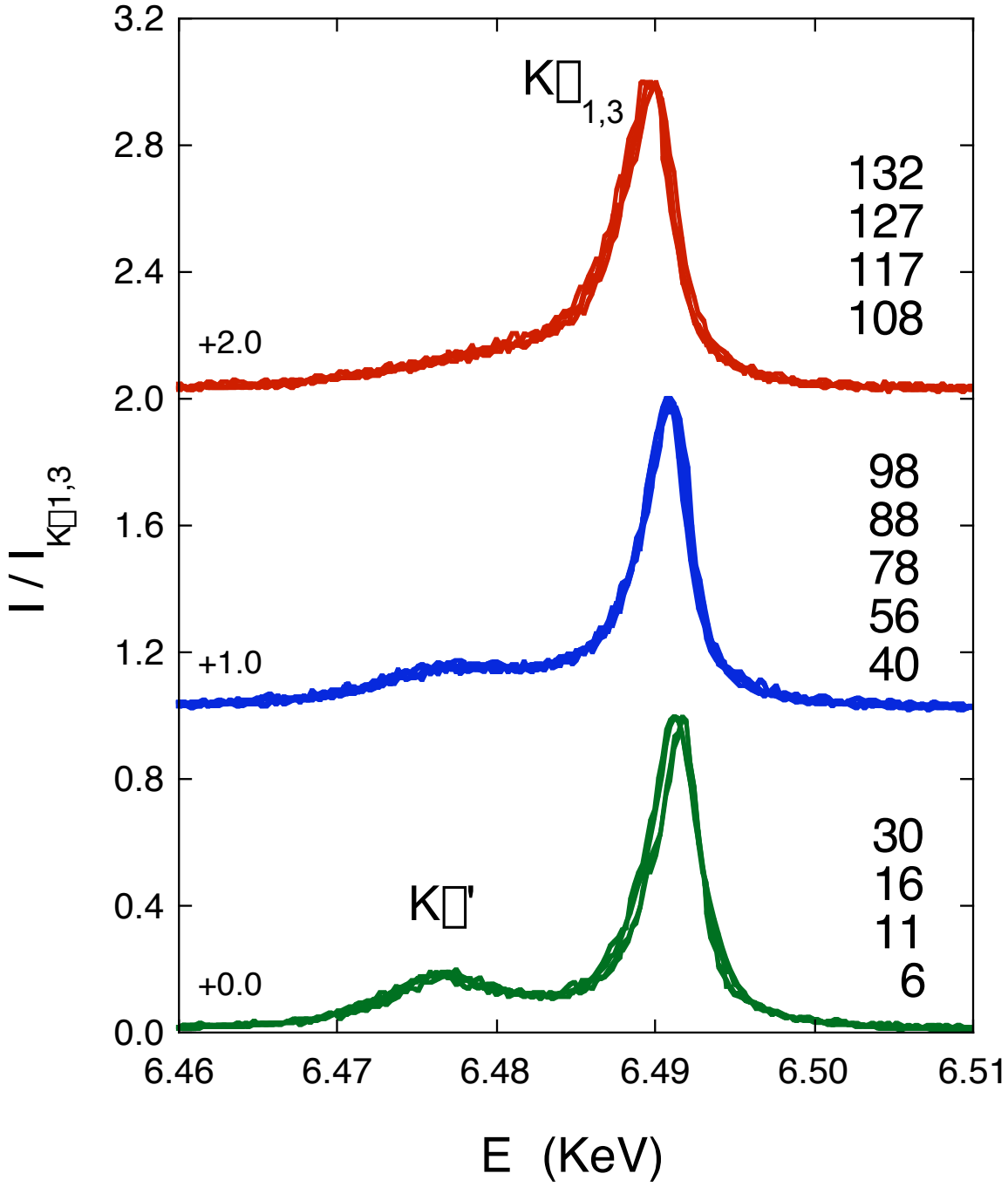
3.2
2.8
2.4
2.0
1.6
1.2
0.8
0.4
0.0
I / I Kα1,3
Kα1,3
Kα'
+2.0
+1.0
+0.0
132
127
117
108
98
88
78
56
40
30
16
11
6
6.46
6.47
6.48
6.49
6.50
6.51
E (KeV)

Fig 1

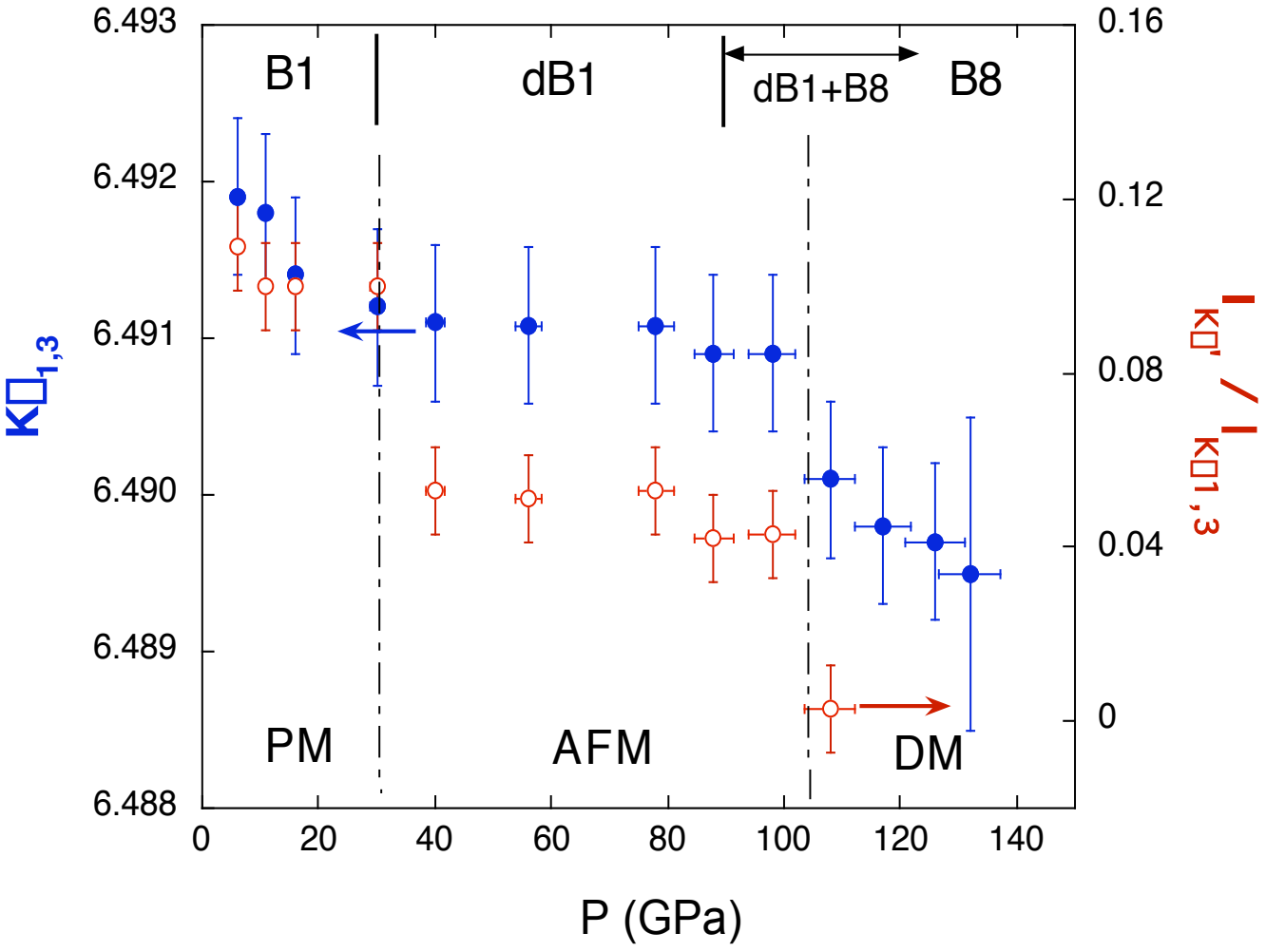
6.493
6.492
6.491
6.490
6.489
6.488
0.16
0.12
0.08
0.04
0
0
20
40
60
80
100
120
140
B1
dB1
dB1+B8
B8
PM
AFM
DM
P (GPa)

Fig 2

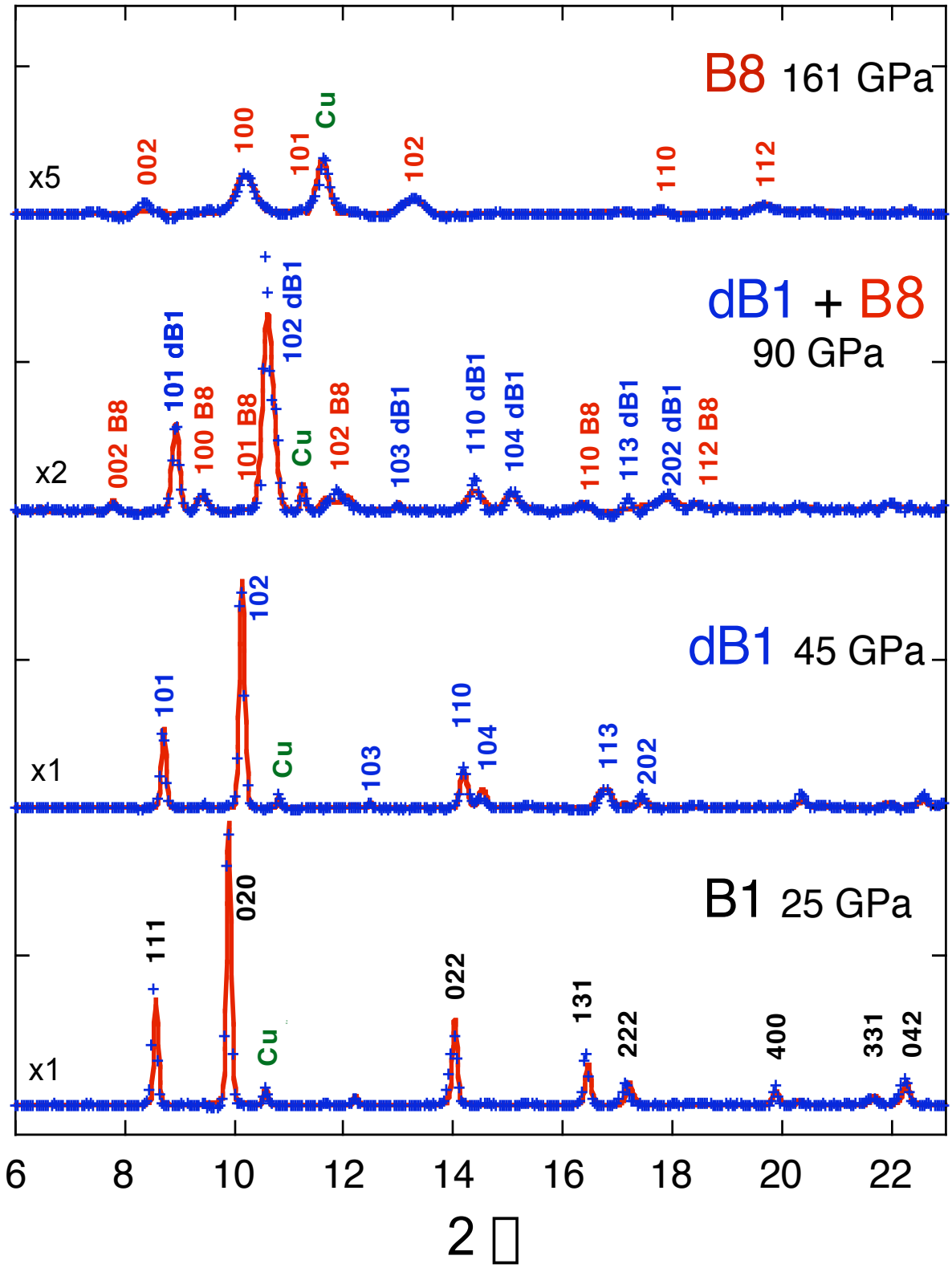
B8 161 GPa
x5
002
100
101
Cu
102
110
112
dB1 + B8
90 GPa
x2
002 B8
101 dB1
100 B8
101 B8
102 dB1
Cu
102 B8
103 dB1
110 dB1
104 dB1
110 B8
113 dB1
202 dB1
112 B8
dB1 45 GPa
x1
101
102
Cu
103
110
104
113
202
B1 25 GPa
x1
111
020
Cu
022
131
222
400
331
042
6
8
10
12
14
16
18
20
22
2θ

Fig. 3

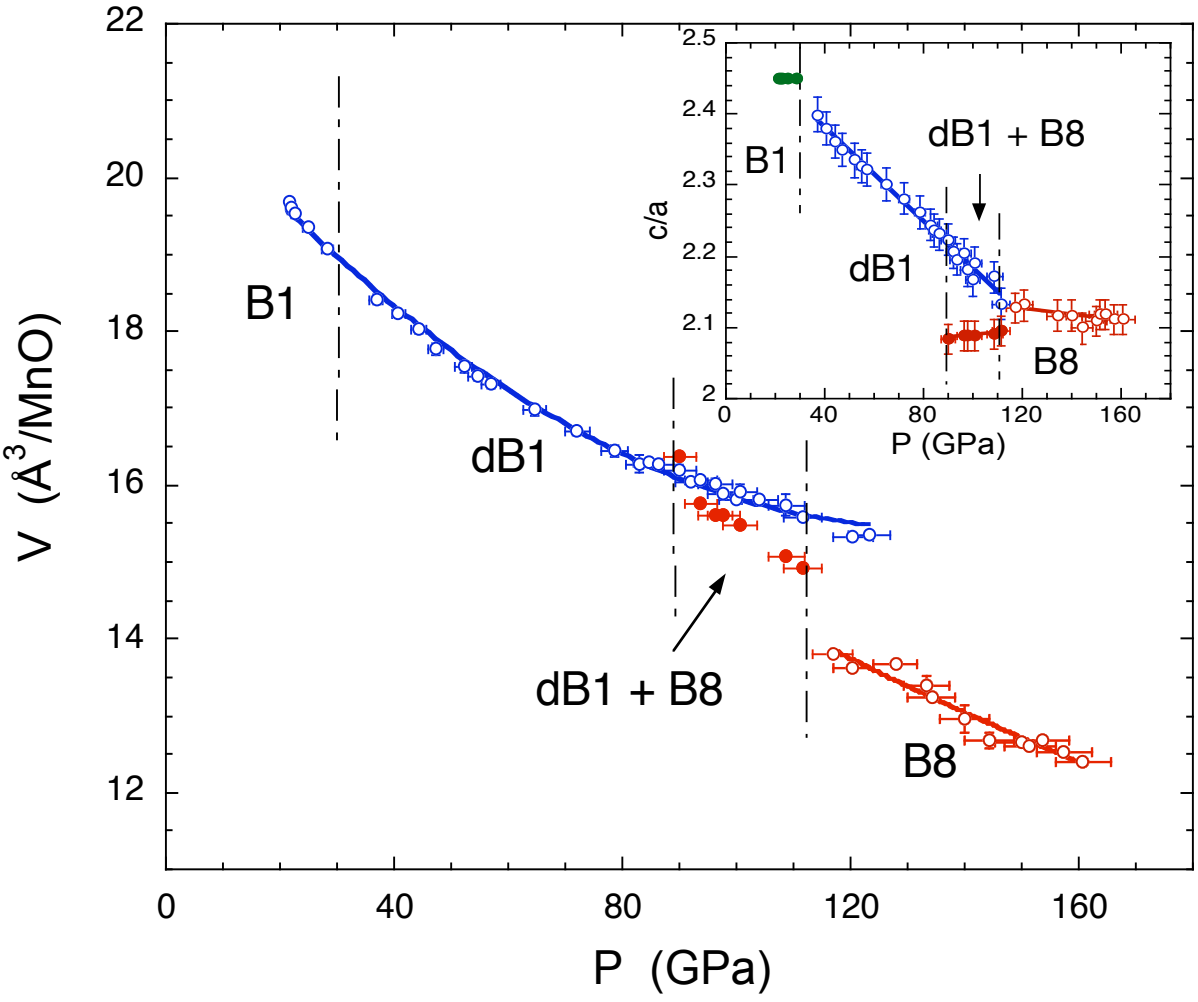

Fig 4